Effect of Aging the Glass of Isotactic Polybutene-1 on Form II Nucleation and Cold Crystallization

ARTICLE *in* THE JOURNAL OF PHYSICAL CHEMISTRY B · NOVEMBER 2013

Impact Factor: 3.3 · DOI: 10.1021/jp4093404 · Source: PubMed

THE JOURNAL OF PHYSICAL CHEMISTRY B

Article

pubs.acs.org/JPCB

Effect of Aging the Glass of Isotactic Polybutene-1 on Form II Nucleation and Cold Crystallization

Isabell Stolte,[†] René Androsch,*[,†] Maria Laura Di Lorenzo,[‡] and Christoph Schick[§]

[†]Center of Engineering Sciences, Martin-Luther-University Halle-Wittenberg, D-06099 Halle/Saale, Germany

[‡]Istituto di Chimica e Tecnologia dei Polimeri (CNR), c/o Comprensorio Olivetti, Via Campi Flegrei, 34, 80078 Pozzuoli (NA), Italy

[§]Institute of Physics, University of Rostock, D-18051 Rostock, Germany

ABSTRACT: The effect of aging initially fully amorphous isotactic polybutene-1 (iPB-1) at temperatures between 243 and 283 K on form II nucleation and cold crystallization has been quantified by fast scanning chip calorimetry. Aging of amorphous iPB-1 at temperatures close to the glass transition temperature leads to formation of nuclei which accelerate subsequent cold crystallization. Analysis of the enthalpy of cold crystallization on heating differently aged samples revealed a maximum rate of nucleation at around 265 K. In contrast, the maximum rate of form II crystallization is observed at distinctly higher temperature of 330−340 K. It is suggested that formation of form II crystal nuclei in the glassy state requires prior densification of the glass since acceleration of cold crystallization on heating the aged glass is detected only after completion of the enthalpy relaxation. The analysis of the rates of nucleation and cold crystallization of iPB-1 at low temperatures is a necessary completion of prior work on the phase transition behavior, and contributes to further understanding of mechanisms of crystal nucleation in polymers.

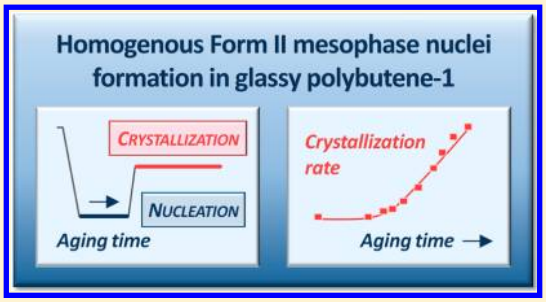

INTRODUCTION

Isotactic polybutene-1 (iPB-1) is a partially crystallizable polymorphic polyolefin with a maximum crystallinity of 50−70%. Cooling the isotropic melt of iPB-1 at atmospheric pressure leads to formation of unstable tetragonal form II crystals which subsequently transform to trigonal form I crystals. The molecular segments adopt a 2*11/3 helix conformation in form II crystals, with large-amplitude intramolecular chain mobility preserved at temperatures above the glass transition temperature of 249 K of the bulk amorphous phase. The form II crystals are therefore classified as conformationally disordered crystals or a mesophase. The density and specific enthalpy of fusion of the form II phase are 0.902 g cm^{-3} and 3.5 kJ mol^{-1}, respectively, and melting at conditions typically applied in standard differential scanning calorimetry (DSC) experiments occurs around 380−390 K.[1−3]

The kinetics of formation of form II crystals from the relaxed melt, their morphology, and higher-order superstructure were extensively investigated in the past as a function of the transformation temperature.[1−14] It has been evidenced that crystals are of lamellar morphology. During their growth, spherulites form with a size which depends on the crystallization temperature. This notwithstanding, it also has been suggested that the crystal morphology, which involves formation of spherulites or quadratic, platelike crystals, depends on both molar mass and transition temperature.[9] Linear growth rates of spherulites are available for temperatures between 303 and 386 K, suggesting a maximum growth rate of around 10^{-6} m s^{-1} at a temperature of 330−340 K. Analysis of the gross crystallization rate revealed a minimum half-time of crystallization of about 1 min, observed at similar temperature; however, data are not available for temperatures lower than 330 K. The temperature dependence of the nucleation density has been estimated by analysis of the number of spherulites and provided information about the nucleation rate. It increases as expected with decreasing temperature in the analyzed temperature range from about 320 to 380 K. As such, the temperature of maximum nucleation rate has not been determined yet, being lower than 320 K.

Due to the relatively high crystallization rate of iPB-1, nucleation and crystallization rates were not yet extensively studied at high supercooling of the melt, at ambient or even lower temperatures. Furthermore, the majority of form II crystallization studies focused on melt crystallization only, that is, on crystallization with the transformation temperature directly approached by cooling the isotropic melt. Regarding cold crystallization, that is, crystallization of the supercooled melt quenched to below the glass transition temperature prior to the approach of the crystallization temperature, it has been found that as-quenched samples revealed no distinct structure larger than 3 nm in the amorphous phase and that heating to room temperature led to formation of microcrystals with a size ranging from 10 to 25 nm.[15,16] Crystallization followed the expected path via form II mesophase formation; however, the form II to form I transition rate was higher in cold-crystallized samples than in air-quenched melt-crystallized samples. It was

Received: September 18, 2013
Revised: November 1, 2013
Published: November 11, 2013

suggested that the higher transformation rate in initially ultraquenched samples was related to the imperfection of the formed microcrystals, as well as the residual stress and free volume frozen in the samples during quenching. It has also been suggested that nucleation/crystallization at high supercooling of the melt may allow direct formation of so-called form I′ crystals, bypassing prior form II crystallization.[1] Early experiments in this field failed; however, it was shown that "passing the sample through the low temperature region has probably resulted in the formation of nuclei of modification I".[1] Note that directly from the melt, solution or during polymerization formed form I′ crystals exhibit an identical crystal structure as form I crystals developing from the form II mesophase, however, are characterized by a higher defect concentration and a lower melting temperature.[17,18] Form I′ crystals also form during strain-induced crystallization, or in the presence of specific nucleating agents, including self-seeding.[19−23] The crystallization rate of the trigonal crystals, even in the presence of specific nuclei, however, is extremely slow, as their lateral growth rate is about 2−3 orders of magnitude slower than the growth rate of tetragonal crystals.[20−24]

It has been shown for numerous polymers including poly(ethylene terephthalate) (PET),[25] poly(L-lactic acid) (PLLA),[26−28] polyamide 6 (PA 6),[29] or isotactic polystyrene (i-PS)[30] that cold crystallization is faster than melt crystallization at identical temperature, caused by the formation of additional crystal nuclei on aging the sample below the cold-crystallization temperature. For iPB-1, such link between the condition of aging below the cold-crystallization temperature, nuclei formation, and the cold-crystallization kinetics has not been established yet, and is therefore the primary object of this work. It is worth noting that melt processing of iPB-1 in industrial processes may involve rapid cooling that enforces form II mesophase formation at high supercooling. This has not been systematically investigated yet regarding the kinetics and the resulting semicrystalline structure/morphology and property profile. For isotactic polypropylene (iPP),[31−36] PA 6,[36−38] or PA 11,[39] it has recently been shown that nucleation of the crystallization process at high supercooling is connected with the development of qualitatively different semicrystalline morphologies than are obtained after nucleation at low supercooling, consequently leading to different material properties.[40−43]

Furthermore, analysis of the nucleation and crystallization behaviors of iPB-1 may provide new insights about the temperature dependence of mechanisms of nucleation. Recent nucleation/crystallization studies of poly(ε-caprolactone) (PCL),[44,45] iPP,[46,47] or PA 11[39] allowed identification of temperature ranges of different nucleation mechanisms. It has been suggested that heterogeneous nucleation, which is evident at rather low supercooling, may be replaced by homogeneous nucleation at high supercooling, with the maximum homogeneous nucleation rate observed around the glass transition temperature. While nucleation/crystallization rates were determined by calorimetry, the suggested change of the nucleation mechanism on variation of the supercooling has been supported by analysis of the morphology and higher-order organization of crystals.[31−39]

EXPERIMENTAL SECTION

In this work, we used a commercial iPB-1 grade PB0110 M from Basell Polyolefins synthesized using a Ziegler−Natta catalyst. The mass-average molar mass and polydispersity are 711 kDa and 6.5, respectively, and the melt flow rate (190 °C, 2.16 kg) is 0.4 g (10 min)$^{-1}$.[48,49]

We used a power-compensation Mettler-Toledo Flash DSC 1 in conjunction with a Huber intracooler TC90. Specimens were prepared by cutting sections of 20−30 μm thickness directly from the pellet using a microtome. The lateral size of the thin section was reduced to about 100 μm, employing a scalpel under a stereomicroscope. The UFS 1 sensor was first conditioned and temperature-corrected according to the specification of the instrument provider, prior to positioning of the specimen in the center of the sample calorimeter. The furnace was permanently purged with dry nitrogen gas at a flow rate of 35 mL min^{-1}. The sample mass of 730 (±70) ng was estimated by comparing the measured absolute heat capacity of fully liquid iPB-1 with the expected specific heat capacity available in the ATHAS database,[50] and comparing the measured with the expected heat-capacity increment on heating a fully amorphous sample at the glass transition temperature. The uncertainty of the sample mass of about 10% controls the uncertainty for the determination of the heat of fusion.[51] Therefore, absolute values of heat of fusion typically are not better than ±15%. For a given sample, however, the reproducibility is distinctly better (±5%), with the error mainly controlled by the uncertainty of the peak integration.

A similar situation occurs for the temperature measurement. The absolute temperature is within ±5 K while peak positions are reproducible better than ±1 K for a given sample. The temperature gradient across a 20 μm thick sample is reported elsewhere.[52,53] For 10 and 20 μm thick polymer samples the thermal lag is about 1 and 2 ms, respectively. At a scanning rate of 10^2 K s^{-1}, this results in a temperature gradient of less than 0.2 K for a 20 μm thick sample which can be neglected. Further details about the instrument/sensor are reported elsewhere.[54−57]

RESULTS AND DISCUSSION

Kinetics of Isothermal Melt and Cold Crystallization. Figure 1 contains temperature−time profiles for isothermal analysis of the kinetics of melt crystallization (left) and cold crystallization (right). In case of melt crystallization, the sample has directly been cooled from 433 K to the analysis temperature

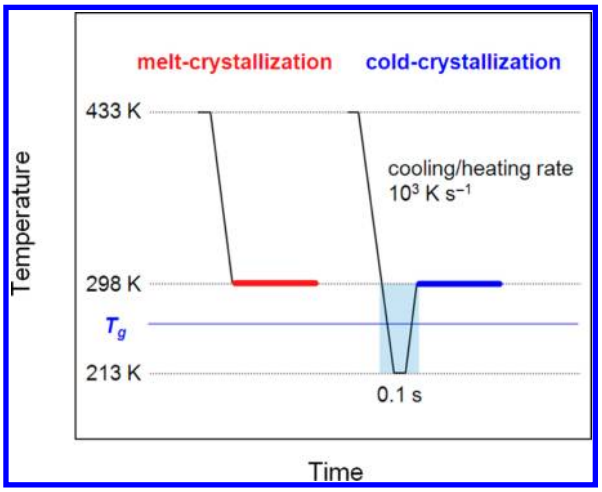

Figure 1. Temperature−time program of FSC experiments applied for analysis of the kinetics of melt crystallization (left) and cold crystallization (right).

dx.doi.org/10.1021/jp4093404 | J. Phys. Chem. B 2013, 117, 15196−15203

at a rate of 10^3 K s^{-1}. In the case of cold crystallization, in contrast, the sample was first cooled to 213 K, kept there for a period of 0.1 s, and then reheated to the crystallization temperature. Crystallization rates were quantified by the half-time of crystallization, determined by interruption of the crystallization process at predefined time, and measurement of the corresponding enthalpy of melting on subsequent fast heating at 10^2 K s^{-1}. Due to the fast heating, cold-ordering and reorganization are avoided and, thus, the enthalpy of melting is equal to the enthalpy of prior isothermal crystallization. Plotting the enthalpy of crystallization as a function of the crystallization time yields conversion−time curves, used for determination of the half-time of crystallization.

The blue-shaded part of the temperature−time program for cold-crystallization experiments indicates the expected temperature/time range for formation of additional crystal nuclei which then may accelerate the overall crystallization process. It is evident that the number of forming nuclei depends on the specific temperature−time profile used, that is, the rates of cooling and heating, the minimum temperature, and residence time at the minimum temperature. In the following, the conditions of cold crystallization summarized in Figure 1 serve as a reference for later discussion of the aging-controlled cold-crystallization behavior.

Figure 2 shows half-times of crystallization of iPB-1 as a function of the crystallization temperature. The red and blue coloring of symbols indicate melt and cold crystallization, respectively, according to the temperature−time profiles shown in Figure 1. Both data sets show a minimum which is expected from the theory of polymer crystallization.[58,59] Melt crystallization (red symbols) is fastest at about 330 K while the maximum of the cold-crystallization rate is observed at slightly higher temperature. Data obtained by FSC (squares) are in agreement with data obtained by DSC (diamond symbols) as well as data available in the literature.[1,2] Important in the context of the present work, it is pointed out that cold crystallization at the chosen reference conditions, shown in Figure 1, is distinctly faster than melt crystallization. This is attributed to the additional residence time of the sample at temperatures lower than the transformation temperature. However, this observation is only true for crystallization temperatures higher than 315 K; at lower temperature, melt- and cold-crystallization rates are identical. Apparently, melt- and cold-crystallization processes at temperatures lower than 315 K, at the specified conditions shown in Figure 1, rely on the instantaneous formation of nuclei, independent of the path the temperature is approached, pointing to a homogeneous nucleation mechanism at the crystallization temperature.

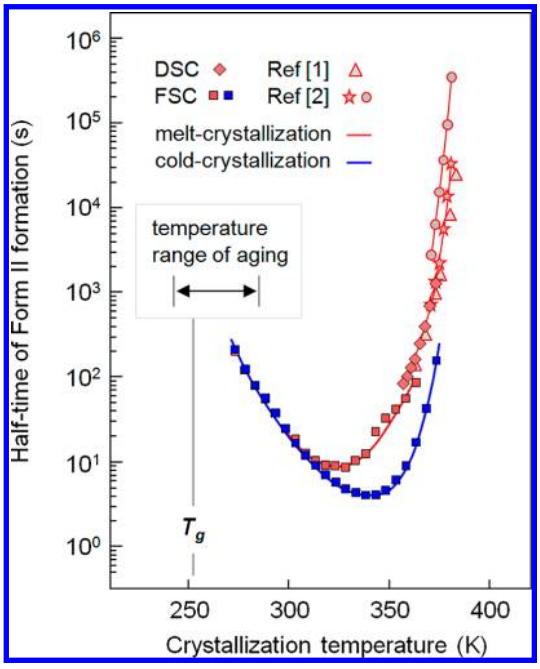

Figure 2. Half-times of crystallization of iPB-1 as a function temperature. The red- and blue-colored symbols indicate melt and cold crystallization, respectively, according to the temperature−time profiles shown in Figure 1. Gray-filled symbols/data were adapted from the literature.[1,2]

It is emphasized that the data of Figure 2 refer to formation of form II mesophase but not form I crystallization. Regarding melt crystallization, represented with the red data points, it has been evidenced by wide-angle X-ray scattering (WAXS) that also in case of high supercooling of the melt first develops form II mesophase before its subsequent transformation into form I crystals.[60,61] Regarding cold crystallization, the early posed suggestion of formation of form I′ nuclei at low temperatures close to T_g,[1] has not been confirmed by later WAXS analysis of the structure of samples which have been ultraquenched into the glassy state and then reheated above T_g for crystallization/ordering.[15] Analysis of the melting behavior of samples melt- and cold-crystallized at identical temperatures showed that their melting temperatures are identical. We consider this as a further proof that the nucleation pathway, as are different on melt and cold crystallization, does not suppress form II formation.

Effect of Low-Temperature Aging on Isothermal Cold Crystallization. It has been emphasized that the kinetics of cold crystallization is controlled by the specific thermal history of the samples. The data of Figure 2 (blue squares) refer to rates of cooling and heating of 10^3 K s^{-1}, a minimum temperature of 213 K, and residence time there of 0.1 s. These conditions control the number of forming crystal nuclei which then may grow at elevated temperature. With increasing number of simultaneously growing nuclei/crystals, the gross crystallization rate is increasing. For evaluation of the effect of the nucleation pathway on the cold crystallization, samples have systematically been aged at temperatures between 243 and 283 K, with the temperature range indicated in Figure 2. Note that the glass transition temperature (T_g), obtained on cooling the melt at a rate of 10^3 K s^{-1}, is observed around 252 K. In other words, the temperature range of aging also includes the glassy state.

In Figure 3 are shown half-times of crystallization as a function of the time of aging amorphous iPB-1 at 258 K, that is, at a temperature 5−10 K higher than T_g. In fact, samples were cooled at 10^3 K s^{-1} to 213 K, kept there for 0.1 s, heated at 10^3 K s^{-1} to the aging temperature, and then recooled to 213 K. After a dwell time of 0.1 s, samples were heated at a rate of 10^3 K s^{-1} to 303, 323, 343, or 368 K to permit cold crystallization. The data of Figure 3 show that aging for a period of time of close to 2 s, or less, does not affect the kinetics of cold crystallization at the chosen reference condition shown in Figure 1. If the aging time, however, exceeds about 2 s, in all cold-crystallization experiments an acceleration of the phase transformation can be observed. After aging for 10^2 s the half-time of cold crystallization is decreased by about 1 order of magnitude. Note again that the half-time of form II mesophase

dx.doi.org/10.1021/jp4093404 | J. Phys. Chem. B 2013, 117, 15196−15203

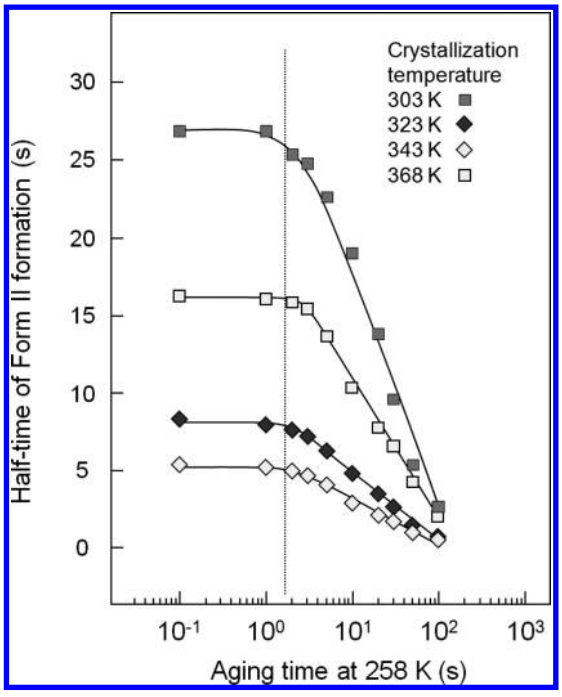

Figure 3. Half-time of cold crystallization of iPB-1 at 303, 323, 343, and 368 K as a function of time of prior aging at 258 K.

formation is minimum around 340 K; that is, at both lower and higher temperatures the half times are increased.

Selected data of Figure 3 were replotted in Figure 4 as a function of temperature, for visualization of the effect of aging

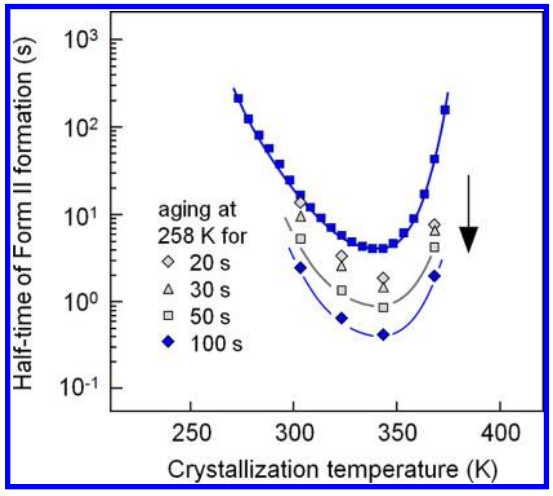

Figure 4. Half-times of cold crystallization of iPB-1 as a function of temperature and pathway of crystal nucleation. The blue squares represent half-times of cold crystallization of samples subjected to the reference-nucleation pathway shown in Figure 1. The gray-colored symbols and blue diamond symbols represent half-times of crystallization of samples which were aged at 258 K for 20, 30, 50, or 100 s, respectively, before cold crystallization at elevated temperature.

on the temperature dependence of the cold-crystallization rate. The blue squares represent half-times of cold crystallization of samples subjected to the reference-nucleation pathway shown in Figure 1, that is, of nonaged samples. The gray-colored symbols and the blue diamond symbols represent half-times of crystallization of samples which were aged at 258 K for 20, 30, 50, or 100 s, respectively, before cold crystallization at elevated temperature. Indicated by the downward trend, it can be seen that aging of amorphous iPB-1 at 258 K leads to an increase of the cold-crystallization rate/decrease of the half-time of cold crystallization in the entire temperature range analyzed, depending on the aging time.

Effect of Low-Temperature Aging on Nonisothermal Cold Crystallization. The analysis of the effect of low-temperature aging on nonisothermal cold crystallization is demonstrated with Figures 5–9. Figure 5 shows apparent

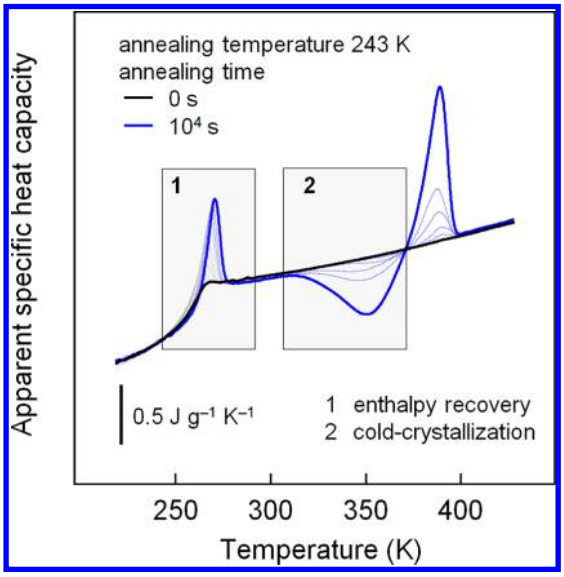

Figure 5. Apparent specific heat capacity of iPB-1 of different thermal history as a function of temperature, obtained on heating at a rate of 10^2 K s^{-1}. All samples were initially rapidly cooled at 10^3 K s^{-1} to 213 K, and then annealed at 243 K for different periods of time between 0 and 10^4 s, as indicated in the legend. Annealing below T_g leads to enthalpy relaxation and nuclei formation which, on heating, is detected with the enthalpy-recovery peak (1), and cold-crystallization peak (2), respectively.

specific heat capacity data of iPB-1 of different thermal history recorded on heating at a rate of 10^2 K s^{-1}. The various curves were obtained after cooling the iPB-1 melt to 213 K and subsequent aging at 243 K, that is, below T_g, for different periods of time between 0 (black curve) and 10^4 s (blue curve). Regardless of the aging conditions, before the beginning of the heating experiment the samples were completely amorphous; that is, aging at 243 K did not result in crystallization within the time frame of the aging experiment, as detailed below. The curve of nonaged iPB-1 shows with the heat-capacity increment at around 255 K the glass transition; however, on continued heating neither exothermic cold crystallization nor endothermic melting is observed. As such, heating at 10^2 K s^{-1} is sufficiently fast to avoid cold crystallization in the absence of previously formed nuclei, being a prerequisite for analysis of the nucleation kinetics at low temperature.[44,45] With increasing aging time up to 10^2 s, we observed first relaxation of the enthalpy which leads on heating to an endothermic enthalpy-recovery peak in conjunction with the glass transition. In Figure 5, the enthalpy-recovery peak is indicated with the gray box labeled "1". Aging for periods of time longer than 10^2 s is connected with the formation of crystal nuclei which causes on heating exothermic cold crystallization, labeled "2" in Figure 5. On continuation of heating, crystals formed during cold crystallization melt around

dx.doi.org/10.1021/jp4093404 | J. Phys. Chem. B 2013, 117, 15196–15203

380 K. Since the areas of the cold-crystallization peak and melting peak for a sample of given annealing history are identical, it is concluded that crystals were absent at the beginning of the heating experiment.

Quantitative data about the enthalpy recovery at the glass transition and the enthalpy of cold crystallization is provided with Figure 6. It shows the areas of the enthalpy-recovery peak

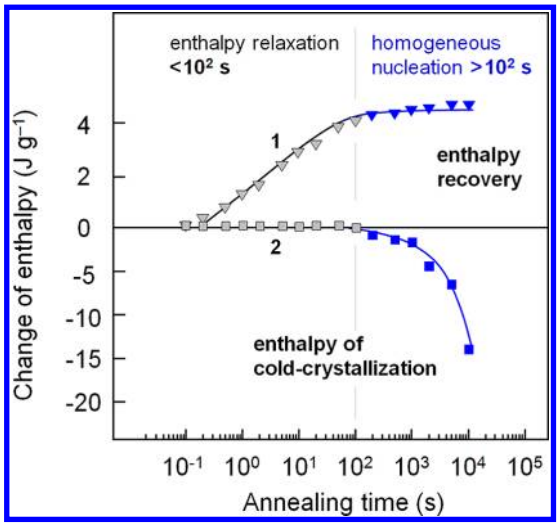

Figure 6. Areas/enthalpies of the enthalpy-recovery peak (top part, curve 1) and cold-crystallization peak (bottom part, curve 2) of the FSC curves obtained on iPB-1 of different thermal history shown in Figure 5, with the data plotted as a function of the time of annealing at 243 K.

(top part) and the cold-crystallization peak (bottom part) as a function of the time of aging at 243 K. The area of the enthalpy-recovery peak, determined as the area between the curves for the nonannealed sample (0 s, black) and the sample under consideration in the temperature range "1", increases with increasing aging time to reach a plateau value after about 10^2 s. The obtained maximum enthalpy change is 4−5 J g^{-1} which is in accord with the maximum expected enthalpy of relaxation of the iPB-1 glass at 243 K. The latter amounts to about 4 J g^{-1} and is determined as $[\approx \Delta c_p \times (T_g - T_a) = 0.41$ J g^{-1} $K^{-1} \times (253 - 243)$ K$]$,[62] with T_a and Δc_p being the annealing temperature and the heat capacity difference of solid and liquid iPB-1 at T_g, respectively. Fast vitrification of the supercooled liquid is connected with the formation of a glass of high enthalpy, which relaxes during aging, connected with a lowering of the enthalpy, ultimately approaching the enthalpy of the liquid at the particular temperature of 243 K. On subsequent heating, devitrification of the relaxed glass is contiguously followed by an endothermic enthalpy-recovery peak.

Cold crystallization in Figure 6 is quantified as the area between the curves for the nonannealed sample (0 s, black) and the sample under consideration in the temperature range "2". The data of Figure 6 reveal that cold crystallization is only observed if the area of the enthalpy-recovery peak is nearly constant and has reached its expected maximum value. In other words, formation of crystal nuclei at 243 K only occurs if the enthalpy relaxation/densification of the glass is completed. At 243 K, which is about 10 K below the T_g observed on cooling at 10^3 K s^{-1}, this is reached already after 10^2 s. The short time originates from the fact that 243 K is only about 6 K below the conventional T_g of about 249 K, measured at 10 K min^{-1}, causing high molecular mobility. The densification proceeds via cooperative segmental motions as long as there is a driving force. After densification of the amorphous phase, eventually the cooperative segmental mobility vanishes because there is no enthalpy difference remaining which otherwise acts as the driving force.[62] If the enthalpy reached the value of the hypothetic liquid phase at identical temperature, then the cooperative segmental mobility slows down and the corresponding relaxation time reaches the value according the Vogel−Fulcher−Tamman law.[63] We observed that nuclei formation only occurs if the densification of the glass is finished; it is about 2 orders of magnitude faster than the remaining cooperative segmental motions,[44] which implies that the formation of small clusters of parallel aligned molecule segments, that is, of crystal nuclei, occurs without the requirement of the cooperative segmental mobility. In other words, the ongoing cooperative segmental motions on length scales of a few nanometers during densification prevent formation or destroy just formed supercritical nuclei, which seem to appear on even smaller length scales.[64] This interpretation of the link between the enthalpy relaxation of the glass and the formation of crystal nuclei presumes a homogeneous nucleation mechanism, similar as it has been suggested in a study of the nucleation and crystallization behavior of PCL.[44]

The effect of aging initially fully amorphous iPB-1 at temperatures slightly above T_g is demonstrated with Figures 7 and 8. Figure 7 shows apparent specific heat capacity data of

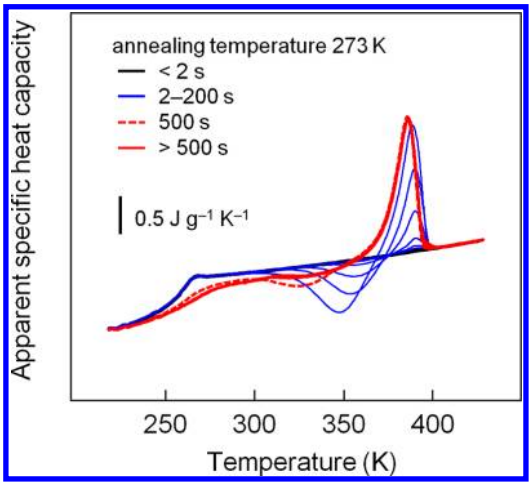

Figure 7. Apparent specific heat capacity of iPB-1 of different thermal history as a function of temperature, obtained on heating at a rate of 10^2 K s^{-1}. All samples were initially rapidly cooled at 10^3 K s^{-1} to 213 K, and then annealed at 273 K for different periods of time, as is indicated in the legend.

initially amorphous iPB-1 which was aged at 273 K for different periods of time, as is indicated in the legend. The black curves were obtained on samples which had been aged at 273 K for periods of time up to 2 s. The data reveal with the steplike increase of the heat capacity the glass transition at about 255 K; however, on increasing the temperature, no further thermal events are seen, leading to the conclusion that both nucleation and crystal growth were not initiated. If the annealing time is between 2 and 200 s (blue curves) then, besides the glass transition at 255 K, exothermic cold crystallization followed by

dx.doi.org/10.1021/jp4093404 | J. Phys. Chem. B 2013, 117, 15196−15203

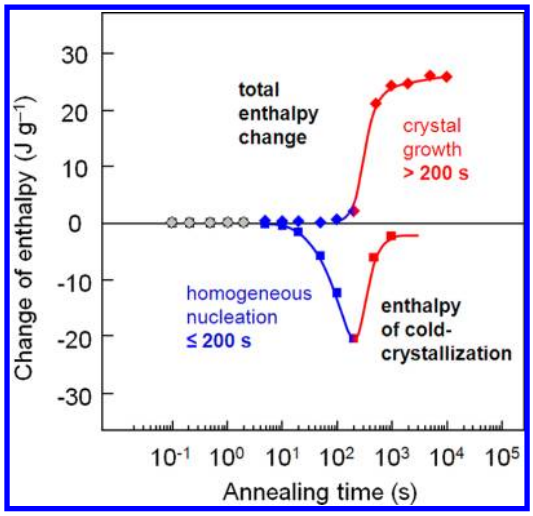

Figure 8. Enthalpy of cold crystallization (squares) on heating iPB-1 of different thermal history at a rate of 10^2 K s^{-1}, plotted as a function of the time of prior annealing at 273 K (bottom part). The top part shows the total change of the enthalpy during annealing at 273 K (diamond symbols). Blue and red coloring of symbols indicate time ranges of annealing at which formation of homogeneous crystal nuclei and crystal growth is observed, respectively.

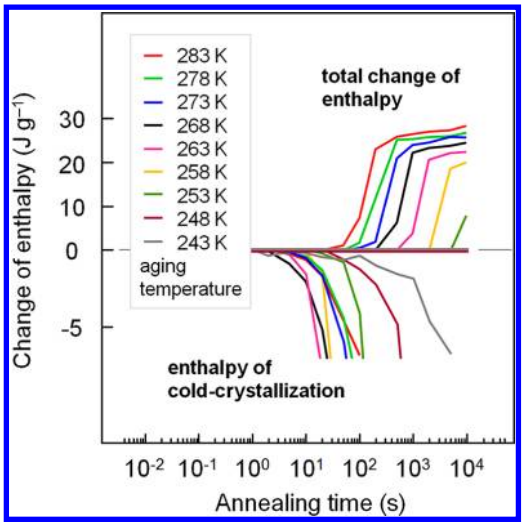

Figure 9. Enthalpy of cold crystallization on heating iPB-1 of different thermal history at a rate of 10^2 K s^{-1}, plotted as a function of the time of prior annealing at different temperatures, as is indicated in the legend (bottom part). The top part shows the total change of the enthalpy during annealing at the various temperatures as a function of the annealing time.

endothermic melting is detected. The heat-capacity increment on devitrification of the glass and equal areas of the cold-crystallization and melting peaks prove that, before the beginning of the FSC heating scan, samples were fully amorphous. Cold crystallization is caused by the formation of crystal nuclei during aging, with the area of the cold-crystallization peak being proportional to the number of nuclei formed. Further increase of the time of aging beyond 200 s leads to crystallization. The heat-capacity increment at T_g is reduced to about 2/3 of the value expected for a fully amorphous sample, and the glass transition range becomes wider and moves to higher temperature after aging for more than 500 s at 273 K. Moreover, cold crystallization is almost completely absent, and the observed total change in enthalpy is related to crystals which were formed during annealing.

Quantitative analysis of the FSC curves of Figure 7 is provided with Figure 8 that visualizes the area of the cold-crystallization peak (bottom part) and total change of the enthalpy during aging at 273 K as a function of the time of aging (top part). The total enthalpy change on heating is determined in the temperature range from 280 to 400 K as the integral of the difference between the measured curve and a linear baseline connecting the integration limits. The gray-colored symbols at aging times less than 2 s indicate that neither cold crystallization/nuclei formation during aging nor crystallization occurred. Aging between 2 and 200 s, indicated by the blue coloring of symbols, leads to cold crystallization/formation of crystal nuclei; however, crystal growth during aging is not detected since the total enthalpy change remains equal to zero. Only if the aging time exceeds 100 s then crystallization is observed, being in accordance with the half-times of crystallization shown in Figure 2. It is worthwhile noting that the area of the cold-crystallization peak decreases as crystallization proceeds during annealing for times longer than 200 s.

In analogy to the experiments and data evaluation explained with Figures 5−8, in Figure 9 are shown the total change of the enthalpy (top part) and the enthalpy of cold crystallization (bottom part) of iPB-1 aged at different temperatures as a function of the time of annealing. The top set of data shows that with decreasing aging temperature, within the frame of the analyzed temperature range from 243 to 283 K, the curves are shifted to longer time; that is, the crystallization rate decreases. This result is expected from the cold-crystallization experiments of Figure 2 which revealed a maximum cold-crystallization rate at about 340 K. Analysis of the cold-crystallization behavior as a function of the time and temperature of aging, provided with the bottom set of curves in of Figure 9, reveals that the nucleation rate is maximum at temperatures distinctly lower than 283 K. Aging at 263 and 268 K leads to cold crystallization on heating as a result of nuclei formation already after aging for 2−3 s. In contrast, if aging is performed at both lower and higher temperatures, then the aging time to observe cold crystallization/nuclei formation is increased.

■ CONCLUSIONS

Survey of the literature regarding the crystallization behavior of iPB-1 revealed that the phase transition of the melt to form II crystals has not yet been fully described and analyzed. In particular, there were not available data about the kinetics of both nucleation and crystallization of the melt at high supercooling, that is, at temperatures close to T_g. This lack of knowledge needs to be attributed to insufficient cooling capacities of analytical instruments to perform studies of the phase transformation kinetics at temperatures lower than the temperature of the maximum crystallization rate.

In the first part of this work, the dependence of the gross crystallization rate on temperature has been analyzed in a wide temperature range between 273 and 373 K, completing earlier work in this field which yielded data at temperatures higher than the temperature of maximum crystallization rate only. According to the results shown in Figure 2, the minimum half-time of melt crystallization is close to 10 s, observed at about 325 K. For the first time, the temperature dependence of the kinetics of cold crystallization, with the samples subjected to defined thermal histories, has been analyzed. As a function of

dx.doi.org/10.1021/jp4093404 | J. Phys. Chem. B 2013, 117, 15196−15203

the specific conditions of aging of iPB-1 samples, cold crystallization occurs distinctly faster than melt crystallization due to the formation of additional crystal nuclei at temperatures lower than the cold-crystallization temperature (Figures 2−4).

Quantitative information about the kinetics of formation of crystal nuclei were collected by analysis of FSC heating scans obtained on iPB-1 of different aging histories. The FSC scans of samples aged below T_g were evaluated regarding the enthalpy recovery peak caused by prior enthalpy relaxation/densification of the glass and regarding the cold-crystallization peak related to prior formation of crystal nuclei. It has been found the formation of crystal nuclei in glassy iPB-1 only occurs after completion of the enthalpy relaxation of the glass, similar to what has been observed for PCL in an independent study.[44] The link between the enthalpy relaxation of the glass and crystal nucleation is interpreted as pointing to a homogeneous nucleation process. Analysis of the aging-time dependence of the enthalpy of cold crystallization on heating of samples aged at different temperatures leads to the conclusion that the rate of nucleation is maximal at around 265 K, a temperature where growth is already significantly slowed down because of the reduced segmental mobility. In contrast, the maximum rate of form II crystallization is observed at the distinctly higher temperature of 330−340 K.

AUTHOR INFORMATION

Corresponding Author

*Phone: +49 3461 46 3762. Fax: +49 3461 46 3891. E-mail: rene.androsch@iw.uni-halle.de.

Notes

The authors declare no competing financial interest.

ACKNOWLEDGMENTS

Financial support by the Deutsche Forschungsgemeinschaft (DFG, AN 212/12) is greatly acknowledged.

REFERENCES

(1) Boor, J., Jr.; Mitchell, J. C. Kinetics of Crystallization and a Crystal-Crystal Transition in Poly-1-butene. *J. Polym. Sci., Part A* **1963**, *1*, 59−84.

(2) Danusso, F.; Gianotti, G. Isotactic Polybutene-1: Formation and Transformation of Modification 2. *Makromol. Chem.* **1965**, *88*, 149−158.

(3) Androsch, R.; Di Lorenzo, M. L.; Schick, C.; Wunderlich, B. Mesophases in Polyethylene, Polypropylene, and Poly(1-butene). *Polymer* **2010**, *51*, 4639−4662.

(4) Monasse, B.; Haudin, J. M. Morphologies and Regimes of Growth of Polybutene Crystals in Phase II. *Macromol. Symp.* **1988**, *20−21*, 295−302.

(5) Tsu, T.-C.; Geil, P. H. Permanganic Etching of Polybutene-1. *Polym. Commun.* **1990**, *31*, 105−108.

(6) Jiang, S.; Duan, Y.; Li, L.; Yan, D.; Chen, E.; Yan, S. An AFM Study on the Structure and Melting Behavior of Melt-Crystallized Isotactic Poly(1-butene). *Polymer* **2004**, *45*, 6365−6374.

(7) Silvestre, C.; Cimmino, S.; Di Lorenzo, M. L. Crystallization of Poly(1-butene)/Hydrogenated Oligocyclopentadiene Blends. *J. Appl. Polym. Sci.* **1999**, *71*, 1677−1690.

(8) Cimmino, S.; Di Lorenzo, M. L.; Silvestre, C. Thermal and Morphological Analysis of Isotactic Poly(1-butene)/Hydrogenated Oligocyclopentadiene Blends. *Thermochim. Acta* **1998**, *321*, 99−109.

(9) Fu, Q.; Heck, B.; Strobl, G.; Thomann, Y. A. A Temperature- and Molar Mass-Dependent Change in the Crystallization Mechanism of Poly(1-butene): Transition from Chain-Folded to Chain-Extended Crystallization? *Macromolecules* **2001**, *34*, 2502−2511.

(10) Icenogle, R. C. Temperature-Dependent Melt Crystallization Kinetics of Poly(butene-1): A New Approach to the Characterization of the Crystallization Kinetics of Semicrystalline Polymers. *J. Polym. Sci., Polym. Phys.* **1985**, *23*, 1369−1391.

(11) Kishore, K.; Vasanthakumari, R. Nucleation Parameters for Polymer Crystallization from Non-Isothermal Thermal Analysis. *Colloid Polym. Sci.* **1988**, *266*, 999−1002.

(12) Braun, J.; Pillichshammer, D.; Eder, G.; Janeschitz-Kriegl, H. Industrial Solidification Processes in Polybutene-1. Part I − Quiescent Melts. *Polym. Eng. Sci.* **2003**, *43*, 180−187.

(13) Yamashita, M. Kinetic Roughening Transition and Missing Regime Transition of Melt Crystallized Polybutene-1 Tetragonal Phase: Growth Kinetics Analysis. *Front. Chem. Eng. China* **2009**, *3*, 125−134.

(14) Erä, V.; Jauhiainen, T. Thermal Analysis of Poly-1-butene. *Angew. Makromol. Chem.* **1975**, *43*, 157−165.

(15) Hsu, C. C.; Geil, P. H. Structure and Properties of Polybutylene Crystallized from the Glassy State. I. X-ray Scattering, DSC, and Torsion Pendulum. *J. Macromol. Sci., Phys.* **1986**, *B25* (4), 433−466.

(16) Hsu, C. C.; Geil, P. H.; Miyaji, H.; Asai, K. Structure and Properties of Polybutylene Crystallized from the Glassy State. II. Electron Microscopy. *J. Macromol. Sci., Phys.* **1986**, *B25* (4), 467−485.

(17) Boor, J., Jr.; Youngman, E. A. Polymorphism in Poly-1-butene: Apparent Direct Formation of Modification I. *J. Polym. Sci., Polym. Lett.* **1964**, *2*, 903−907.

(18) Rakus, J. P.; Mason, C. D. The Direct Formation of Modification I′ Polybutene-1. *J. Polym. Sci., Polym. Lett.* **1966**, *4*, 467−468.

(19) Petermann, J.; Gohil, R. M. A New Method for the Preparation of High Modulus Thermoplastic Films. *J. Mater. Sci.* **1979**, *14*, 2260−2264.

(20) Gohil, R. M.; Miles, M. J.; Petermann, J. On the Molecular Mechanism of the Crystal Transformation (Tetragonal-Hexagonal) in Polybutene-1. *J. Macromol. Sci. Phys.* **1982**, *21*, 189−201.

(21) Yamashita, M.; Hoshino, A.; Kato, M. Isotactic Poly(butene-1) Trigonal Crystal Growth in the Melt. *J. Polym. Sci., Polym. Phys.* **2007**, *45*, 684−697.

(22) Yamashita, M. Direct Crystal Growth of Isotactic Polybutene-1 Trigonal Phase in the Melt: *In-situ* Observation. *J. Cryst. Gr.* **2008**, *310*, 1739−1743.

(23) Yamashita, M. Crystal Growth Kinetics and Morphology of *Isotactic* Polybutene-1 Trigonal Phase in the Melt. *J. Cryst. Growth* **2009**, *311*, 560−563.

(24) Di Lorenzo, M. L.; Righetti, M. C.; Wunderlich, B. Influence of Crystal Polymorphism on the Three-Phase Structure and on the Thermal Properties of Isotactic Poly(1-butene). *Macromolecules* **2009**, *42*, 9312−9320.

(25) Illers, K.-H. Geordnete Strukturen in "amorphem" Polyäthylenterephthalat. *Kolloid. Z. Z. Polym.* **1971**, *245*, 393−398.

(26) De Santis, F.; Pantani, R.; Titomanlio, G. Nucleation and Crystallization Kinetics of Poly(lactic acid). *Thermochim. Acta* **2011**, *522*, 128−134.

(27) Sánchez, M. S.; Mathot, V. B. F.; Vanden Poel, G.; Ribelles, J. L. G. Effect of Cooling Rate on the Nucleation Kinetics of Poly(L-lactic acid) and its Influence on Morphology. *Macromolecules* **2007**, *40*, 7989−7997.

(28) Androsch, R.; Di Lorenzo, M. L. Crystal Nucleation in Glassy Poly(L-lactic acid). *Macromolecules* **2013**, *46*, 6048−6056.

(29) Kolesov, I.; Androsch R. *Proceedings, 29th Annual Meeting Polymer Processing Society (PPS), July 15−19, 2013, Nuremberg, Germany*; Androsch, R. Manuscript in preparation.

(30) Cheng, S. Z. D.; Lotz, B. Enthalpic and Entropic Origins of Nucleation Barriers During Polymer Crystallization: The Hoffman−Lauritzen Theory and Beyond. *Polymer* **2005**, *46*, 8662−8681.

(31) Hsu, C. C.; Geil, P. H.; Miyaji, H.; Asai, K. Structure and Properties of Polypropylene Crystallized from the Glassy State. *J. Polym. Sci., Polym. Phys.* **1986**, *24*, 2379−2401.

(32) Ogawa, T.; Miyaji, H.; Asai, K. Nodular Structure of Polypropylene. *J. Phys. Soc. Jpn., Lett.* **1985**, *54*, 3668−3670.

(33) Piccarolo, S. Morphological Changes in Isotactic Polypropylene as a Function of Cooling Rate. *J. Macromol. Sci., Phys.* **1992**, *B31*, 501−511.
(34) Zia, Q.; Androsch, R.; Radusch, H.-J.; Piccarolo, S. Morphology, Reorganization, and Stability of Mesomorphic Nanocrystals in Isotactic Polypropylene. *Polymer* **2006**, *47*, 8163−8172.
(35) Zia, Q.; Radusch, H.-J.; Androsch, R. Direct Analysis of Annealing of Nodular Crystals in Isotactic Polypropylene by Atomic Force Microscopy, and its Correlation with Calorimetric Data. *Polymer* **2007**, *48*, 3504−3511.
(36) van Drongelen, M.; Meijer-Vissers, T.; Cavallo, D.; Portale, G.; Vanden Poel, G.; Androsch, R. Microfocus Wide-Angle X-ray Scattering of Polymers Crystallized in a Fast Scanning Chip Calorimeter. *Thermochim. Acta* **2013**, *563*, 33−37.
(37) Mileva, D.; Kolesov, I.; Androsch, R. Morphology of Cold-ordered Polyamide 6. *Colloid Polym. Sci.* **2012**, *290*, 971−978.
(38) Mileva, D.; Androsch, R.; Zhuravlev, E.; Schick, C. Morphology of Mesophase and Crystals of Polyamide 6 Prepared in a Fast Scanning Chip Calorimeter. *Polymer* **2012**, *53*, 3994−4001.
(39) Mollova, A.; Androsch, R.; Mileva, D.; Schick, C.; Benhamida, A. Effect of Supercooling on Crystallization of Polyamide 11. *Macromolecules* **2013**, *46*, 828−835.
(40) Zia, Q.; Androsch, R.; Radusch, H.-J. Effect of the Structure at the Micrometer and Nanometer Scale on the Light Transmission of Isotactic Polypropylene. *J. Appl. Polym. Sci.* **2010**, *117*, 1013−1020.
(41) Zia, Q.; Radusch, H.-J.; Androsch, R. Deformation behavior of isotactic polypropylene crystallized via the mesophase. *Polym. Bull.* **2009**, *63*, 755−771.
(42) Mileva, D.; Zia, Q.; Androsch, R. Tensile Properties of Random Copolymers of Polypropylene with Ethylene and 1-Butene: Effect of Crystallinity and Crystal Habit. *Polym. Bull.* **2010**, *65*, 623−634.
(43) Kolesov, I.; Mileva, D.; Androsch, R. Mechanical Behavior and Optical Transparency of Polyamide 6 of Different Morphology Formed by Variation of the Pathway of Crystallization. *Polym. Bull.* DOI: 10.1007/s00289-013-1079-9.
(44) Zhuravlev, E.; Schmelzer, J. W. P.; Wunderlich, B.; Schick, C. Kinetics of Nucleation and Crystallization in Poly(ε-caprolactone). *Polymer* **2011**, *52*, 1983−1997.
(45) Wurm, A.; Zhuravlev, E.; Eckstein, K.; Jehnichen, D.; Pospiech, D.; Androsch, R.; Wunderlich, B.; Schick, C. Crystallization and Homogeneous Nucleation Kinetics of Poly(ε-caprolactone) (PCL) with Different Molar Masses. *Macromolecules* **2012**, *35*, 3816−3828.
(46) Silvestre, C.; Cimmino, S.; Duraccio, D.; Schick, C. Isothermal Crystallization of Isotactic Poly(propylene) Studied by Superfast Calorimetry. *Macromol. Rapid Commun.* **2007**, *28*, 875−881.
(47) Mileva, D.; Androsch, R.; Zhuravlev, E.; Schick, C.; Wunderlich, B. Homogeneous Nucleation and Mesophase Formation in Glassy Isotactic Polypropylene. *Polymer* **2012**, *53*, 277−282.
(48) Hadinata, C. "Flow-induced Crystallization of Polybutene-1 and Effect of Molecular Parameters". Ph.D. Thesis, Melbourne, 2007.
(49) Product information, available at https://polymers.lyondellbasell.com.
(50) Advanced Thermal Analysis System data bank, available at http://www.springermaterials.com/docs/athas.html.
(51) Zhuravlev, E.; Schick, C. Fast Scanning Power Compensated Differential Scanning Nano-calorimeter: 2. Heat Capacity Analysis. *Thermochim. Acta* **2010**, *505*, 14−21.
(52) Minakov, A. A.; Adamovsky, S. A.; Schick, C. Non Adiabatic Thin-Film (Chip) Nanocalorimetry. *Thermochim. Acta* **2005**, *432*, 177−185.
(53) Zhuravlev, E.; Schick, C. Fast Scanning Power Compensated Differential Scanning Nano-calorimeter: 1. The device. *Thermochim. Acta* **2010**, *505*, 1−13.
(54) Mathot, V.; Pyda, M.; Pijpers, T.; Vanden Poel, G.; van de Kerkhof, E.; van Herwaarden, S.; van Herwaarden, F.; Leenaers, A. The Flash DSC 1, a Power Compensation Twin-type, Chip-based Fast Scanning Calorimeter (FSC): First Findings on Polymers. *Thermochim. Acta* **2011**, *522*, 36−45.
(55) van Herwaarden, S.; Iervolino, E.; van Herwaarden, F.; Wijffels, T.; Leenaers, A.; Mathot, V. Design, Performance and Analysis of Thermal Lag of the UFS1 Twin-Calorimeter Chip for Fast Scanning Calorimetry Using the Mettler-Toledo Flash DSC 1. *Thermochim. Acta* **2011**, *522*, 46−52.
(56) Iervolino, E.; van Herwaarden, A. W.; van Herwaarden, F. G.; van de Kerkhof, E.; van Grinsven, P. P. W.; Leenaers, A. C. H. I.; Mathot, V. B. F.; Sarro, P. M. Temperature Calibration and Electrical Characterization of the Differential Scanning Calorimeter Chip UFS1 for the Mettler-Toledo Flash DSC 1. *Thermochim. Acta* **2011**, *522*, 53−59.
(57) Vanden Poel, G.; Istrate, D.; Magon, A.; Mathot, V. Performance and Calibration of the Flash DSC 1, a New, MEMS-Based Fast Scanning Calorimeter. *J. Therm. Anal. Calorim.* **2012**, *110*, 1533−1546.
(58) Hoffmann, J. D.; Davis, G. T.; Lauritzen, J. I. The rate of crystallization of linear polymers with chain folding. In *Treatise on solid state chemistry, crystalline and noncrystalline solids*; Hannay, H. B., Ed.; Plenum Press: New York, 1976; Vol. *3*.
(59) Wunderlich, B. Macromolecular Physics. In *Crystal nucleation, growth, annealing*; Academic Press: New York, 1976; Vol. *2*.
(60) Azzurri, F.; Alfonso, G. C.; Gomez, M. A.; Marti, M. C.; Ellis, G.; Marco, C. Polymorphic transformation in isotactic 1-butene/ethylene copolymers. *Macromolecules* **2004**, *37*, 3755−3762.
(61) Chau, K. W.; Yang, Y. C.; Geil, P. H. Tetragonal → Twinned Hexagonal Crystal Phase Transformation in Polybutene-1. *J. Mater. Sci.* **1986**, *21*, 3002−3104.
(62) Hodge, I. M. Enthalpy Relaxation and Recovery in Amorphous Materials. *J. Non-Cryst. Solids* **1994**, *169*, 211−266.
(63) Vogel, H. Das Temperaturabhängigkeitsgesetz der Viskosität. *Phys. Z.* **1921**, *22*, 645−646.
(64) Donth, E. *Glass Transition*; Springer: Berlin, 2001.